THE JOURNAL OF BIOLOGICAL CHEMISTRY VOL. 287, NO. 8, pp. 5891–5897, February 17, 2012
© 2012 by The American Society for Biochemistry and Molecular Biology, Inc. Published in the U.S.A.

Engineering Upper Hinge Improves Stability and Effector Function of a Human IgG1[S]

Received for publication, October 11, 2011, and in revised form, December 9, 2011 Published, JBC Papers in Press, December 27, 2011, DOI 10.1074/jbc.M111.311811

Boxu Yan[‡1], Daniel Boyd[‡], Timothy Kaschak[‡], Joni Tsukuda[§], Amy Shen[§], Yuwen Lin[¶], Shan Chung[¶], Priyanka Gupta[‖], Amrita Kamath[‖], Anne Wong[**], Jean-Michel Vernes[**], Gloria Y. Meng[**], Klara Totpal[‡‡], Gabriele Schaefer[‡‡], Guoying Jiang[§§], Bartek Nogal[‡], Craig Emery[‡], Martin Vanderlaan[§§], Paul Carter[¶¶], Reed Harris[§§], and Ashraf Amanullah[‡]

From the [‡]Department of Pharma Technical Development, Genentech, Oceanside, California 92056 and the Departments of [§]Early Stage Cell Culture, [¶]Bioanalytical Science, [‖]Pharmacokinetics and Pharmacodynamics, [**]Assay and Automation Technology, [‡‡]Immunology, [§§]Analytical Development & Quality Control, and [¶¶]Antibody Engineering, Genentech, San Francisco, California 94080

Background: Radical reactions result in breakage of the heavy-light chain linkage and hinge cleavage of an IgG1.
Results: The degraded products are generated by different reaction pathways and mechanisms.
Conclusion: A His^{229}/Tyr substitution improves stability and effector function of an IgG1.
Significance: A mechanism based strategy to engineer the upper hinge to improve multiple properties of an IgG1 is feasible.

Upper hinge is vulnerable to radical attacks that result in breakage of the heavy-light chain linkage and cleavage of the hinge of an IgG1. To further explore mechanisms responsible for the radical induced hinge degradation, nine mutants were designed to determine the roles that the upper hinge Asp and His play in the radical reactions. The observation that none of these substitutions could inhibit the breakage of the heavy-light chain linkage suggests that the breakage may result from electron transfer from Cys^{231} directly to the heavy-light chain linkage upon radical attacks, and implies a pathway separate from His^{229}-mediated hinge cleavage. On the other hand, the substitution of His^{229} with Tyr showed promising advantages over the native antibody and other substitutions in improving the stability and function of the IgG1. This substitution inhibited the hinge cleavage by 98% and suggests that the redox active nature of Tyr did not enable it to replicate the ability of His to facilitate radical induced degradation. We propose that the lower redox potential of Tyr, a residue that may be the ultimate sink for oxidizing equivalents in proteins, is responsible for the inhibition. More importantly, the substitution increased the antibody's binding to FcγRIII receptors by 2–3-fold, and improved ADCC activity by 2-fold, while maintaining a similar pharmacokinetic profile with respect to the wild type. Implications of these observations for antibody engineering and development are discussed.

Recombinant monoclonal antibodies (mAbs)[2] have been established as promising therapeutic agents with more than 20 mAbs approved by the Food and Drug administration in various indications in the past two decades (1). With the accumulating knowledge and experience with this class of therapeutics, more effort has been focused on exploring and extending the variety of antibody structures that can improve product quality and efficacy to better serve patients (2–8). The fact that nearly all marketed antibody drugs are in the IgG format and most contain a human Fc region of the IgG1 isotype suggests that the focus on human mAbs, in particular IgG1, is likely to intensify through future research and development. However, the application of antibody engineering strategies to all mAbs tends to be limited, as structure or modifications may be optimized for one mAb, but may compromise another *in vivo* (6). Thus, a mechanism-based strategy for engineering mAbs to improve multiple properties and/or functions should be more successful in delivering the development and manufacturing goals.

The integrity of the upper hinge Asp^{226}-Lys-Thr-His-Thr is important for an IgG1, as it may impact product safety, efficacy, and even production yield as mAbs are susceptible to H_2O_2 generated in *in vivo* environments as well as in the cell culture production media. The lack of understanding of the mechanisms governing many product quality and stability attributes suggests a new direction needs to be explored. Recent studies of radical reaction induced degradation sheds light on the human IgG1 upper hinge (9–11). The hinge degradation induced by hydroxyl radical (•OH) attack results in a variety of products under different reaction conditions (Fig. 1) (9, 11). Under high oxygen tension, the hinge cleavage releases degraded products consisting of a Fab domain and a partial IgG1 that is missing the Fab, and these products are characterized by a ladder of the C-terminal heavy chain residues in the Fab complementary to the N-terminal ladder of one of the heavy chains of the Fc domain in the truncated IgG1. However, under low oxygen tension, products are generated at a slower rate, about the same as those derived from the breakage of the heavy-light chain linkage, leading to either cleavage of the peptide bond between Cys^{225} and Ser^{224} to yield a light chain (LC) and Fab portion of the heavy chain (HC), or just releasing a LC without any cleavage of peptide bond (Fig. 1). Although our previous observa-

[S] This article contains supplemental Figs. S1 and S2.

[1] To whom correspondence should be addressed. E-mail: byan1027@gmail.com.

[2] The abbreviations used are: mAb, monoclonal antibody; ET, electron transfer; ADCC, antibody-dependent cell-mediated cytotoxicity; PK, pharmacokinetics; DHFR, dihydrofolate reductase; SEC, size exclusion chromatography; ADC, antibody drug conjugate.

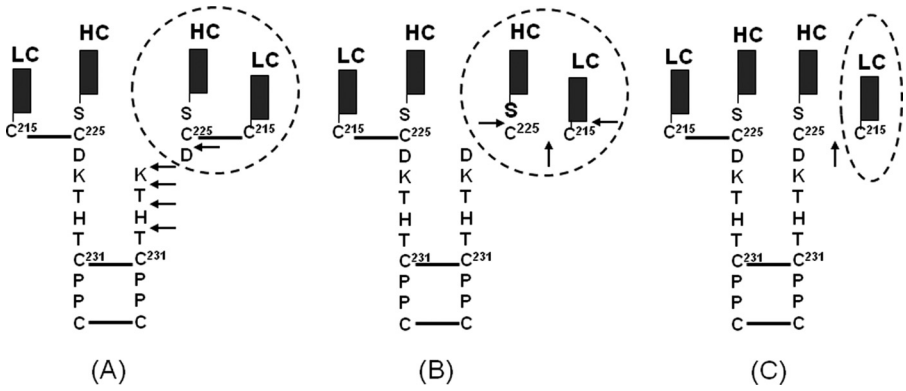

FIGURE 1. **Schematic illustration of the ˙OH radical induced hinge degradation in a human IgG1.** The ˙OH radicals induce degradations of an IgG1 hinge to generate different products under different conditions. Under high oxygen tension, hinge cleavage releases Fab fragment and a partial IgG1 that is missing the Fab, with complementary ladders of C- and N-terminal hinge residues (Asp^{226}, Lys^{227}, Thr^{228}, His^{229}, and Thr^{230}) of the upper hinge (*panel A*) (9); whereas under low oxygen tension, breakage of the heavy-light chain linkage leads to the peptide bond cleavage that releases light chain (LC) and Fab portion of the heavy chain (HC) (*panel B*), or the breakage of the heavy chain (HC) and light chain (LC) linkage without any cleavage of peptide bond (*panel C*) (11). The hinge degradation is initiated by radical formation at Cys^{231} resulting from breakage of the first hinge disulfide bond between two heavy chains by the ˙OH attacks, and followed by radical reactions via ET and localization onto the upper hinge or the inter-chain disulfide bond. The degraded products (*circled*) varies depending on the reaction conditions, as described previously (9–11).

tions demonstrated the critical role of His^{229} in the radical reactions as its imidazole ring enables the His^{229} to function as a transient radical center, it remains unclear if the various degradation products are generated by different reaction pathways or are just function of different by oxygen tensions.

It has been known that electron transfer (ET) plays an important role in radical driven reactions, as the electron can tunnel from one center to another when encountering other nearby redox centers (12–14), suggesting that the localization of the electron could be the critical step to determine what products would be generated. Our previous observations suggested that distance from the radical center and reaction rate constants may determine yields in the cleavage sites of the upper hinge residues (9–10). However, these factors did not fully rationalize the reason why substitutions of the His^{229} with Ser, Gln, and Ala all block the hinge cleavage, as Ala does not form a hydrogen bond that is required for the ET. To address these questions, the unique characteristics of the upper hinge that is framed by two disulfide bond pairs of the HC-HC bond and LC-HC bond need to be further evaluated for their roles in the ET and radical reaction mechanism. For example Asp^{226}, which is capable of forming a hydrogen bond with His^{229}, may play an important role in electron transfer (ET) of the radical reaction mechanism (10). In addition, it remains unclear if the His^{229} also drive the breakage of the HC-LC linkage, as substitution of His^{229} with Ala dramatically promoted the breakage (10). Information obtained from these new assessments would be very important for antibody development. To this end, a combination of studies is necessary to address the potential impacts of these residues to product quality, pharmacokinetics (PK) and effector functions, such as antibody-dependent cell-mediated cytotoxicity (ADCC), because significant effects to the ADCC from hinge substitutions have been observed previously (15).

In this study, we present the results from evaluating nine mutants of the upper hinge that revealed new insights into the radical reaction mechanism. Consistent with our previous observations for the key role of His^{229}, the results suggest that the breakage of the HC-LC linkage and cleavage of the hinge may follow different pathways, driven by Cys^{231} and His^{229}, respectively. In addition, our results show that Asp^{226} maybe not critical for the radical reactions, whereas substitution of His with Tyr reveals a potential strategy for improving stability and function of the IgG1: it maintains a similar pharmacokinetic profile with respect to the native molecule and increases the antibody binding to FcγRIII receptors by 2–3-fold, and improves ADCC activity by 2-fold. In combination with our previous observations (10), these results demonstrate the feasibility of engineering the upper hinge to improve the stability and effector function of the IgG1.

EXPERIMENTAL PROCEDURES

Generation of the Upper Hinge Variants—Substitutions were generated by site-directed mutagenesis. Dihydrofolate reductase (DHFR)-deficient CHO cells were transfected using Lipofectamine 2000 CD according to the manufacturer's recommendation (Invitrogen). Transfected cells were centrifuged and seeded into DMEM/F-12-based selective (glycine-, hypoxanthine-, and thymidine-free) medium containing various concentrations of MTX to get individual colonies. A few weeks after seeding, individual colonies from each MTX concentration were picked into a 96-well plate for ELISA assay for antibody titer. Top clones were scaled-up based on antibody titers to produce each mutant using proprietary chemically defined production medium employing a 14-day fed-batch and temperature shift process in shake flask. The Harvested Cell Culture Fluid (HCCF) from each mutant was chromatographically purified using protein-A affinity chromatography, for a few mutants that showed a higher level of high molecular weight species (HMW), cation-exchange chromatography was applied to decrease remove the HMW level to below 2%. All samples were subjected to an endotoxin determination to ensure product quality before *in vivo* studies.

Characterization of the Mutants and Native mAbs by in Vitro Assays—The native IgG1 and its mutants were incubated with 20 mM H_2O_2 at 25 °C in 1× phosphate-buffered saline buffer, pH 7.4. Characterization of these products were carried out

according to the procedures described previously (9, 10). Briefly, the degraded products were separated by size exclusion chromatography (SEC) on TSK G3000SWxl dual columns, 7.8 × 300 mm, at a flow rate of 0.5 ml/min. Eluting protein was monitored at 280 nm. The light chain released by radical reactions was determined by reversed-phase high performance liquid chromatography (RP-HPLC) and in line time of flight mass spectrometry (TOF/MS) under non-reducing conditions. RP-HPLC was performed on an Agilent 1200 HPLC system. The mobile phase included water with 0.11% trifluoroacetic acid as solvent A and acetonitrile (Burdick Jackson) with 0.09% TFA as solvent B. A Varian PLRP-S (Varian, Inc., Palo Alto, CA), 4.6 × 50 mm, 8 μm particle size, 1000-Å pore size column was used for the RP-HPLCTOF/MS analysis. The column eluent was analyzed by UV detection at 215 nm and then directed in-line to a TOF mass spectrometer. The separation was performed at 75 °C at a flow rate of 0.5 ml/min. Electrospray ionization TOF/MS was performed on an Applied Biosystems QSTAR Elite XL mass spectrometer. The electrospray ionization mass spectra were analyzed using BioAnalyst protein deconvolution software (Applied Biosystems).

ELISA Assays for FcγR Binding and FcRn Binding—These assays were performed using FcγR and FcRn expressing CHO cells, as described previously (16). Binding of to Fc receptors was measured by enzyme-linked immunosorbent assay (ELISA). For FcγR binding, 384-well ELISA plates were coated with anti-glutathione *S*-transferase followed by addition of the extracellular domain fused with Gly-His_6-glutathione *S*-transferase at the C terminus. Serially diluted IgG (for FcγRI binding) or IgG complexed with anti-human antibody (for FcγRII and FcγRIII binding) were added to the plates. Bound IgG was detected with horseradish peroxidase (HRP)-labeled goat $F(ab')_2$ anti-human IgG $F(ab')_2$. For FcRn binding, 96-well ELISA plates were coated with NeutrAvidin followed by biotinylated FcRn. Serially diluted IgG in pH 6.0 buffer was added. Bound IgG was detected with HRP-labeled goat $F(ab')_2$ anti-human IgG $F(ab')_2$. For evaluation of dissociation at pH 7.4, bound IgG was subjected to an additional incubation step at pH 7.4. Then the detection antibody was added.

In Vivo Characterization of the Mutants—Twelve female SCID beige mice were assigned to each of six groups (n = 12/group) and given a single intravenous (IV) bolus dose of 2 or 25 mg/kg of the IgG1, mutant 4 or mutant 9. Serum samples were collected at various time points up to 21 days post-dose and analyzed for the IgG1, Mutant 4, or Mutant 9 concentrations using an ELISA method. The ELISA method consisted of a HER1 ECD capture reagent and a horseradish peroxidase (HRP)-labeled goat Fab'2 anti-human Fc detection reagent. Serum concentration-time profiles were used to estimate the following PK parameters using non-compartmental analysis (WinNonlin, version 5.2.1; Pharsight Corporation, Mountain View, CA): total drug exposure defined as area under the serum concentration time curve extrapolated to infinity (AUCinf), clearance (CL), volume of distribution at steady state (Vss), observed maximum serum concentration (Cmax) and terminal half-life (T1/2λ). A naïve pooled approach was used to provide one estimate for each treatment group.

ADCC Assay—ADCC assays were carried out using peripheral blood mononuclear cells (PBMCs) from healthy human donors as effector cells and A431 cells as target cells as described previously (17). To minimize inter-donor variability derived from allotypic differences at residue 158 position in FcγRIII, blood donors were limited to those carrying the heterozygous FcγRIII genotype (F/V158). Target cells in 50 μl of assay medium (RPMI 1640 with 1% BSA and 100 units/ml penicillin and streptomycin) were seeded in a 96-well, round-bottom plate at 4×10^4/well. Serial dilutions of test and control antibodies (50 μl/well) were added to the plates containing the target cells, followed by incubation at 37 °C with 5% CO_2 for 30 min to allow opsonization. The final concentrations of antibodies ranged from 10,00 to 0.004 ng/ml following 4-fold serial dilutions for a total of 10 data points. After the incubation, 1.0×10^6 PBMC effector cells in 100 μl of assay medium were added to each well to give a ratio of 25:1 effector:target cells, and the plates were incubated for an additional 4 h. The plates were centrifuged at the end of incubation and the supernatants were tested for lactate dehydrogenase (LDH) activity using a Cytotoxicity Detection Kit (Roche Applied Science; Indianapolis, IN). The LDH reaction mixture was added to the supernatants and the plates were incubated at room temperature for 15 min with constant shaking. The reaction was terminated with 1 M H_3PO_4, and absorbance was measured at 490 nm (the background, measured at 650 nm, was subtracted for each well) using a SpectraMax Plus microplate reader (Molecular Devices). Absorbance of wells containing only the target cells served as the control for background (Low Control), whereas wells containing target cells lysed with Triton-X100 provided the maximum signal available (High Control). Antibody-independent cellular cytotoxicity (AICC) was measured in wells containing target and effector cells without the addition of antibody. The extent of specific ADCC was calculated in Equation 1.

$$\%\ \mathrm{ADCC} = 100 \times [A_{490}(\mathrm{Sample}) - A_{490}(\mathrm{AICC})]/[A_{490}(\mathrm{HighControl}) - A_{490}(\mathrm{LowControl})] \quad \text{(Eq. 1)}$$

RESULTS

Substitution Design—Nine substitutions were designed and generated in this study, as shown in Fig. 2*A*. Mutants 1–3 were designed to evaluate the impact of Asp^{226}, following the strategy described in our previous study (10). The Asp^{226} was also assessed by double or triple substitutions in combination with His^{229} and Lys^{227}(mutations 4–6). In addition, substitutions 7 and 8 were designed to test if the "arginine-aspartate (Arg-Asp) salt bridge" (13) could impact degradation, since the rate of ET through a donor-(Arg-Asp)-acceptor salt bridge has been found to be ~40–100 times slower than the corresponding switched interface (13, 20). Meanwhile, prior indications suggest Tyr plays an important role in radical reactions and ET in proteins (12–14), thus, His/Tyr substitution 9 was designed to examine if Tyr could replace His as a transient radical center or play any role in the radical reactions. Structure analysis has revealed that the composition of polar residues confers great

A

Native	SCDKTHTCPPC
Mutant 1	SCSKTHTCPPC
Mutant 2	SCAKTHTCPPC
Mutant 3	SCNKTHTCPPC
Mutant 4	SCSKTSTCPPC
Mutant 5	SCDKTSTCPPC
Mutant 6	SCSSTSTCPPC
Mutant 7	SCDRTHTCPPC
Mutant 8	SCRDTHTCPPC
Mutant 9	SCDKTYTCPPC

B

SEC results of testing the mutants on H_2O_2 induced cleavage

Molecules	% LMW		% change	% Inhibition
	Day 0	Day 6		
Native	0.78	6.80	6.02	
Mutant 1	1.42	5.45	4.03	33
Mutant 2	1.17	6.14	4.97	18
Mutant 3	1.38	7.04	5.66	6
Mutant 4	1.26	1.58	0.32	95
Mutant 5	0.96	1.16	0.30	97
Mutant 6	1.29	1.65	0.36	94
Mutant 7	1.44	6.73	5.29	12
Mutant 8	1.44	4.57	3.13	43
Mutant 9	1.01	1.23	0.22	98

FIGURE 2. **Substitutions in the upper hinge and related impacts to radical induced hinge cleavage.** Nine mutants were designed to determine any roles of Asp^{225} and His^{229} in the hinge cleavage. These substitutions were constructed by introducing single or double substitutions in the upper hinge of the native sequence by site-directed mutagenesis. Substituted residues are *underlined* (*panel A*). These mutants were evaluated for their ability to inhibit the hinge cleavage by SEC to measure the degraded products (Fab and a partial IgG1), the SEC was performed after incubating the IgG1 with H_2O_2 in a molar ratio of 1:200 at 25 °C for 2, 4, and 6 days, respectively. The cleavage products (% LMW) are shown as % of the peak area of the products to the whole molecule in the UV signals (*panel B*). For clarity, only the results from Day 6 and Day 0 are shown here. Percent change was calculated by comparing the level of % LMW at Day 6 to Day 0. Percent inhibition was calculated by the equation: % = (% change of the native − % change of mutant)/% change of the native. *LMW*: low molecular weight species (Fab and a partial IgG1). The results are reported as an average of two replicates.

flexibility to the upper hinge that accommodate the vastly different placements of the two Fab domains relative to the Fc domain (18). Therefore, it was not expected that the substitutions in the upper hinge would negatively impact the conformational stability. This idea is consistent with our previous studies that showed no impact of similar substitutions to FcγR binding and potency of an IgG1 (10), and the results using substitutions 4, 6, and 9 also supported this idea (see below).

Asp Is Not Critical for the Radical Reactions that Impact Stability of the IgG1—Stability of these mutants was first examined by size exclusion chromatography (SEC) to measure degraded products: a cleaved Fab and a partial IgG1 that is missing the Fab. SEC was performed after incubating the IgG1 with H_2O_2 in a molar ratio of 1:200 at 25 °C for 2, 4, and 6 days, respectively. The degraded products were found to accumulate over time, but each of the substitutions exhibited different cleavage rates. The results at day 6 are shown in Fig. 2*B*. It appears that Asp^{226} did not play a critical role in the radical reactions, as substitutions of Asp^{226} did not significantly reduce the hinge cleavage, only produced slight inhibitions (6–33%) as observed in mutants 1–3. In addition, inhibitions of 94–95% observed for a single His^{229} (mutant 5) and substitutions of Asp and Lys in combination with His^{229} (mutants 4 and 6) further demonstrated that Asp^{226} was not critical in the radical reactions.

The possibility that the "salt bridge" may inhibit the hinge cleavage was tested using mutations 7 and 8. The mutant 8 only showed a moderate inhibition of ~40%; the mutant 7, with the potential to form the "salt bridge," showed little inhibition. Although Asp^{226} and Lys^{227} are adjacent in the hinge sequence, crystal structure (18) and modeling structure of an IgG1 hinge (10) revealed that the side chains of these two residues are not aligned in positions conducive to "salt bridge" formation. Considering the similar nature of the side chains in Arg and Lys, it is expected that a similar configuration exists for the Asp-Arg pair in the upper hinge of the mutants. This suggests that the "salt bridge" is unlikely to be formed in the upper hinge.

His^{229}/Tyr Substitution Blocks Radical Induced Hinge Cleavage—Radical reactions induce hinge cleavage of an IgG1, in which His^{229} radical formed by receiving an electron from Cys^{231} initiates the redox chemistry to obtain a proton from its neighboring residue, leading to the hinge cleavage (9, 10). It has been known that Tyr is a redox active residue and has a reaction rate constant of 3.4×10^8 with an electron faster than His at 6.4×10^7 and Ser at $\sim 3 \times 10^7$ (14). Therefore, His/Tyr substitution was tested to determine if Tyr could replace His to function as the transient radical center. The results showed a strong inhibition of the hinge cleavage by ~98% (Fig. 2*B*), suggesting that Tyr does not function like His to facilitate the hinge degradation, rather inhibits the degradation. Similar observations that Tyr functions as a redox-active on or off switch in the ET reactions to mediate protein function were reported previously (13, 21, 22).

Breakage of the HC-LC Linkage Is a Separated Event in the Radical Reactions—Another outcome of the radical reactions in the hinge of an IgG1 is the breakage of the HC-LC linkage (11). To determine if any of the substitutions could inhibit the breakage, the nine mutants were treated with H_2O_2 in a molar ratio of 1:200 at 25 °C for 6 days, then a level of released LC was determined by reversed phase high performance liquid chromatography in line with time of flight mass spectrometry (RP-HPLC-TOF/MS) under non-reducing conditions as described previously (10). The released LC was detected in the range of 3.1–3.5% for these mutants and native molecule (details not shown), suggesting no difference in resisting the breakage between the native and mutant molecules under high oxygen tension. This is consistent with our previous results using the native and the His/Ser and His/Ser +Lys/Ser mutants (10). As mutants 4, 5, 6, and 9 showed strong inhibitions to the hinge cleavage, these mutants and the native IgG1 were further tested for their ability to resist thermal induced cleavage by incubating with 20 μM Cu^{2+} at 37 °C for 15 days. These samples were then characterized by RP-HPLC-TOF/MS, no notable difference between the native one and mutants was detected (details not shown). Altogether, these results suggested that the breakage of the LC-HC linkage may follow a separated reaction pathway or

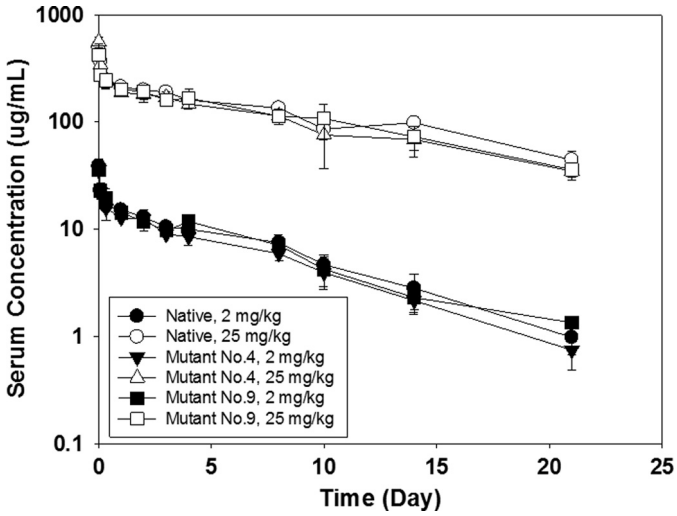

FIGURE 3. **Characterization of mutants 4 (His/Ser+Asp/Ser) and 9 (His/Tyr) for *in vivo* PK profile.** Pharmacokinetics of the native IgG1 and two mutants were characterized by single IV bolus dose in SCID beige mice using 2 or 25 mg/kg of the IgG1. Serum samples were collected at various time points up to 21 days post-dose and analyzed for the IgG1, Mutant 4, or Mutant 9 concentrations that were measured using an ELISA method as described under "Experimental Procedures." Each data point was obtained using 3 mice. These results showed similar PK profiles between the native IgG1 and its mutants.

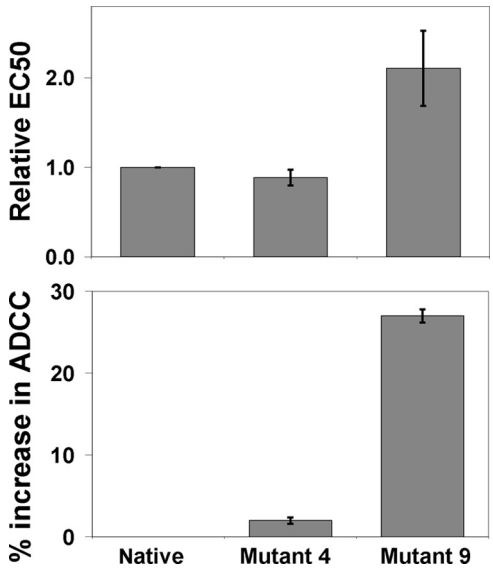

FIGURE 4. **Effect of the substitutions 4 and 9 on ADCC activity of the IgG1.** ADCC assays were carried out using peripheral blood mononuclear cells (PBMCs) from healthy human donors as effector cells and A431 cells as target cells (see "Experimental Procedures" for details). The native IgG1 and its mutants were tested using PBMCs from two donors and a E:T ratio of 25:1 against A431 cells. S.D. are indicated by error bars and represent triplicate measurements within the same experiment. Data shown are representative using PBMCs from 4 different individual donors. These results indicate that the substitution 9 is more potent than the native IgG1 in the ADCC function, while the mutant 4 behaves similarly to the native IgG1.

mechanism different from mechanisms of governing the hinge cleavage that is driven by His^{229} as a transient radical center.

Evaluation of the Potential of Selected Mutants for Improving Quality Attributes and Function of the IgG1—Along with our previous observations (10), these results allow us to hypothesize that an engineered upper hinge may enable IgG1 to resist the radical induced hinge cleavage *in vivo* or in cell culture production conditions, and may improve antibody function as well. To test this hypothesis, Mutants 4, 5, 6, and 9, which showed potential for resisting the hinge cleavage, were first evaluated for manufacturability and production yields. Mutants 4, 6, and 9 outperformed the native protein and mutant 5 with an extra 15–25% yield in titers ($n = 6$) (data not shown). A typical level of <3% of high molecular weight (HMW) species or aggregate was found in mutants 4, 6, 9 and the native IgG1, whereas an unusually high level at 13.6% of HMW species was detected in mutant 5 after protein A chromatography purification. These HMW species consist of a dimmer at ~90% and trimmer at ~10% (not shown), it remains unclear what caused the unusual high level of the HMW, and if it correlates with the lower titer of mutant 5. Nonetheless, these observations suggested that mutants 4, 6, and 9 had high potential for manufacturability and production yields.

Our previous results showed that replacing His^{229} and Lys^{227} with Ser did not change FcγR binding and potency of an IgG1 (10), and current study showed that the mutant 6 (His/Ser +Lys/Ser+ Asp/Ser) behaved similarly to the mutant 4, and considering the potentials of mutants 4 (His/Ser + Asp/Ser) and 9 (His/Tyr) in enhancing hinge stability, thus, the latter two mutants were further evaluated for efficacy in comparison with the native IgG1. PK profiles were obtained by administrating mutants 4, 9, and native proteins into mice by single I.V. injection with a low dose of 2 mg/kg, and a high dose of 25 mg/kg, respectively. The serum antibody concentrations were measured at different time points. As shown in Fig. 3, the PK profiles of the mutants are consistent with the wild type. The clearance rate of the mutant and native proteins is similar, ranging from 8–10 ml/day/kg for the high dosing, and 14–17 ml/day/kg for the low dosing. These observations were in good agreement with the FcRn binding data which showed no significant difference between the mutants and native IgG1 (see supplemental Fig. S1). These results suggest that the PK profile remains intact for these mutated molecules compared with the native molecule.

Many therapeutic mAbs rely on effector function to achieve clinical efficacy, and the ability of mAbs to induce ADCC depends on their binding affinity to both the target and to the activating FcγR (4, 23–25). The results from ELISA based binding assays indicated that while binding to other FcγR receptors remained unchanged for mutant 4 compared with the native, mutant 9 (His/Tyr) had a 3.1 times higher binding to F158 FcγRIII, and 2.2 times higher binding to V158 FcγRIII than the native IgG1, respectively (supplemental Fig. S2). These observations were further confirmed in the ADCC assay (Fig. 4). Mutant 4 behaved similarly to the native IgG1, whereas mutant 9 showed a 27% increase in ADCC activity, and was 2.1 times more potent in EC_{50} than the native one. The His/Tyr substitution in mutant 9 did not change the fucosylation profile as glycan analysis showed no difference from the native IgG1 (not shown), confirming that the enhanced ADCC activity resulted from the His/Tyr substitution. The IgG1 used in this study has a mild ADCC function with an EC_{50} at ~11 ng/ml, and binds to two separate important receptors that are expressed by A431 cells, therefore, our results demonstrated that the His/Tyr sin-

gle substitution in the upper hinge is capable of improving ADCC activity in IgG1.

DISCUSSION

The results presented in this study enhanced our understanding of the radical induced hinge degradation. The hinge cleavage and breakage of the HC-LC linkage may follow different reaction pathways, one is driven by the transient radical center His^{229}, and another may result from an electron localization onto the HC-LC bond that was transferred directly from Cys^{231}. On the other hand, the observed inhibition of the hinge cleavage from the His^{229}/Tyr substitution indicated that Tyr did not facilitate the radical reactions, rather it blocked the cleavage. More importantly, the His/Tyr substitution improved *in vivo* ADCC function and production yield. To our knowledge, this is the first report that the single substitution of the His^{229}/Tyr in the upper hinge could improve stability and ADCC function of an IgG1.

The observed similar levels in the released LC between the native and mutants implies that the His^{229} did not directly involve in the breakage of the HC-LC linkage. As an energy-driven process, an electron transferred from Cys^{231} may directly localize onto the HC-LC bond. The results supporting this idea come from the analysis of the hinge structure (10, 18): one upper hinge region forms a spiral arrangement of residues, and the other forms an extended turn. With the extreme flexibility of the upper hinge, the His^{229} may not align in the position between the Cy^{231} and the HC-LC bond. Thus it is possible for direct transportation of an electron between them, implying a separated pathway from the His^{229} mediated hinge cleavage. This idea is also consistent with our previous observations that no difference in the level of released LC between His/Ser and the native IgG1 was observed (10). Although the distance between Cys^{231} and the HC-LC bond of 16–17 Å is greater than a typical electron tunneling distance of 14 Å (26, 27), a direct transfer of electron is still possible as new local conformation or conformational dynamic in the upper hinge region under thermal dynamic conditions could bring the HC-LC bond more proximal to Cys^{231} to facilitate the radical reactions.

On the other hand, such distance dependent reactions could limit the interaction frequency between Cys^{231} and the HC-LC bond, resulting in a slow production of the degraded fragments, which is consistent with our observations under thermal incubation conditions (11). Thus, these results suggest the breakage of the HC-LC linkage could be driven by a different mechanism separated event from the hinge cleavage in the radical-induced hinge degradation. These results also imply that the breakage of the HC-LC linkage may not be preventable by substitutions in the upper hinge, and substitution of the Cys^{231} of the HC may be needed to inhibit such degradation. From structural point of view, this substitution is not expected to disrupt the function of an IgG1, as the HC and LC can still associate together strongly without a disulfide bond by high binding affinity between them (28). Recent development in antibody drug conjugate (ADC) therapeutics also supports this idea, as these ADC molecules are built by reducing the disulfide bonds in the hinge and conjugating toxins onto the Cys residues, and the modified IgG1 remains fully functional without a disulfide bond (29, 30). It remains to be seen if such a substitution could inhibit the breakage of the HC-LC linkage of an IgG1.

Our results demonstrated the merits for the single His/Tyr substitution in engineering mAbs to improve multiple properties of mAbs. The extreme flexibility of the upper hinge allows the side chains of His^{229} and Cys^{231} to align in positions to allow the ET (10), so that the His^{229} can receive an electron from $Cys^{231}$and functions as the transient radical center. Although both substitutions of His/Ser and His/Tyr blocked the hinge cleavage, they may follow different mechanisms. Compared with Tyr, a slower reaction rate constant of $\sim 3 \times 10^7$ (14) and the less redox active nature of Ser may prevent it from localizing the electron that is the critical step for the hinge cleavage. Different from many observations that Tyr facilitates radical reactions in proteins, its redox active nature and having a faster reaction rate constant than Tyr of 3.4×10^8 (14) did not enable it to replace His, and indeed, the mutant strongly inhibited the hinge cleavage, suggesting some other property of the residue played the critical role in the process. The positive redox potential difference of 0.24 V between His ($E^\circ = 1.17$V) and Cys ($E^\circ = 0.93$V) allows the initial electron transfer from Cys^{231} to His^{229} upon radical attacks, whereas the lower potential of Tyr ($E^\circ = 0.83$V) (14, 21) could sink the electron, stopping it from transferring onto other upper hinge residues. Therefore, we propose that the difference in redox potentials between His and Tyr could be an on/off switch in the ET process that could mediate the hinge cleavage.

The observations that substitutions 4 and 9 increased production yield suggest that ability to inhibit the hinge cleavage may contribute to a higher production of mAb in cell culture conditions. Although some controversies remain about relationship between FcRn affinity and *in vivo* clearance (31, 32), FcRn has been indicated as major factor in regulating IgG homeostasis (33, 34). This may explain the reason why the improved stability profile did not translate into a better PK profile. More importantly, our results demonstrated that these substitutions did not impact *in vivo* PK profile, and that the His/Tyr substitution dramatically improved ADCC function. Rather than achieving improvements in the ADCC function by multiple substitutions (15, 19, 35), our results showed improvement in ADCC function by a single substitution in the upper hinge. Oganesyan *et al.* (35) proposed molecular mechanisms for the improvement in ADCC function by substitutions as they may enhance Fc openness as well as additional molecular interactions at the corresponding interface of Fc and FcγR. Given the location of the His^{229} at the upper hinge, the His/Tyr substitution may enhance the interactions between Fc and FcγR, resulting in improved ADCC function. Collectively, our results demonstrated the feasibility to engineer the upper hinge to improve multiple properties of an IgG1.

With the current trend toward developing targeted therapeutics, the data from clinical trials indicates that mAbs derived from human sequences by various engineering technologies are effective, and are likely to be less immunogenic than those with rodent-derived sequences. As H_2O_2-mediated radical reactions occur in *in vivo* and *in vitro* conditions, the hinge degradation should be considered as a product quality attribute to the development programs for mAbs. Following "Quality by Design"

principles, our results may support a new approach to improve product stability and a cost effective way to generate therapeutic mAbs, and offer a new strategy to enhance effector functions using the His/Tyr substitution. We believe that such mechanism based design and engineering of mAbs would facilitate optimized structure and function, and help us to bring more affordable targeted mAbs to the market.

Acknowledgments—We thank our colleagues in the Department of Analytical Operations for performing glycan analysis, titer assays, and endotoxin experiments, and our colleagues in the IVSG group for assistance in conducting the mouse PK study.

REFERENCES

1. Nelson, A. L., Dhimolea, E., and Reichert, J. M. (2010) Development trends for human monoclonal antibody therapeutics. *Nat. Rev. Drug Discov.* **9,** 767–774
2. Carter, P. J. (2006) Potent antibody therapeutics by design. *Nat. Rev. Immunol.* **6,** 343–357
3. Nelson, A. L., and Reichert, J. M. (2009) Development trends for therapeutic antibody fragments. *Nat. Biotechnol.* **27,** 331–337
4. Beck, A., Wurch, T., Bailly, C., and Corvaia, N. (2010) Strategies and challenges for the next generation of therapeutic antibodies. *Nat. Rev. Immunol.* **10,** 345–352
5. Jefferis, R. (2009) Glycosylation as a strategy to improve antibody-based therapeutics. *Nat. Rev. Drug Discov.* **8,** 226–234
6. Walsh, G., and Jefferis, R. (2006) Post-translational modifications in the context of therapeutic proteins. *Nat. Biotechnol.* **24,** 1241–1252
7. Schneider, C. K., and Kalinke, U. (2008) Toward biosimilar monoclonal antibodies. *Nat. Biotechnol.* **26,** 985–990
8. Reichert, J. M., and Valge-Archer, V. E. (2007) Development trends for monoclonal antibody cancer therapeutics. *Nat. Rev. Drug Discov.* **6,** 349–356
9. Yan, B., Yates, Z., Balland, A., and Kleemann, G. R. (2009) Human IgG1 hinge fragmentation as the result of H2O2-mediated radical cleavage. *J. Biol. Chem.* **284,** 35390–35402
10. Yates, Z., Gunasekaran, K., Zhou, H., Hu, Z., Liu, Z., Ketchem, R. R., and Yan, B. (2010) Histidine residue mediates radical-induced hinge cleavage of human IgG1. *J. Biol. Chem.* **285,** 18662–18671
11. Yan, B., and Boyd, D. (2011) Breaking the light and heavy chain linkage of human immunoglobulin G1 (IgG1) by radical reactions. *J. Biol. Chem.* **286,** 24674–24684
12. Garrison, W. M. (1987) Reaction mechanisms in the radiolysis of peptides, polypeptides, and proteins. *Chem. Rev* **87,** 381–388
13. Reece, S. Y., and Nocera, D. G. (2009) Proton-coupled electron transfer in biology: results from synergistic studies in natural and model systems. *Annu. Rev. Biochem.* **78,** 673–699
14. Davies, M. J., and Dean, R. T (1997) *Radical-mediated Protein Oxidation* pp. 50–120, Oxford University Press, Oxford, U.K.
15. Dall'Acqua, W. F., Cook, K. E., Damschroder, M. M., Woods, R. M., and Wu, H. (2006) Modulation of the effector functions of a human IgG1 through engineering of its hinge region. *J. Immunol.* **177,** 1129–1138
16. Lu, Y., Vernes, J. M., Chiang, N., Ou, Q., Ding, J., , Adams, C., Hong, K., Truong, B. T., Ng, D., Shen, A., Nakamura, G., Gong, Q., Presta, L. G., Beresini, M., Kelley, B., Lowman, H., Wong, W. L., and Meng, Y. G. (2011) Identification of IgG(1) variants with increased affinity to FcγRIIIa and unaltered affinity to FcγRI and FcRn: comparison of soluble receptor-based and cell-based binding assays. *J. Immunol. Methods* **365,** 132–141
17. Shields, R. L., Namenuk, A. K., Hong, K., Meng, Y. G., Rae, J., Briggs, J., Xie, D., Lai, J., Stadlen, A., Li, B., Fox, J. A., and Presta, L. G. (2001) High resolution mapping of the binding site on human IgG1 for Fc γRI, Fc γRII, Fc γRIII, and FcRn and design of IgG1 variants with improved binding to the Fc γR. *J. Biol. Chem.* **276,** 6591–6604
18. Saphire, E. O., Stanfield, R. L., Crispin, M. D., Parren, P. W., Rudd, P. M., Dwek, R. A., Burton, D. R., and Wilson, I. A. (2002) Contrasting IgG structures reveal extreme asymmetry and flexibility. *J. Mol. Biol.* **319,** 9–18
19. Stewart, R., Thom, G., Levens, M., Güler-Gane, G., Holgate, R., Rudd, P. M., Webster, C., Jermutus, L., and Lund, J. (2011) A variant human IgG1-Fc mediates improved ADCC. *Protein Eng. Des. Sel.* **24,** 671–678
20. Kirby, J. P., and Nocera, D. G. (1997) Significant effect of salt bridges on electron transfer. *J. Am. Chem. Soc.* **119,** 9230–9236
21. Mohammad, R., Seyedsayamdost, J. X., Clement, T. Y., Chan, P. G., and Schultz, J. S. (2007) Site-specific insertion of 3-aminotyrosine into subunit α2 of *E. coli* ribonucleotide reductase: direct evidence for involvement of Y730 and Y731 in radical propagation. *J. Am. Chem. Soc.* **129,** 15060–15071
22. Seyedsayamdost, M. R., Yee, C. S., Reece, S. Y., Nocera, D. G., and Stubbe, J. (2006) pH rate profiles of FnY356-R2s (n = 2, 3, 4) in *Escherichia coli* ribonucleotide reductase: evidence that Y356 is a redox-active amino acid along the radical propagation pathway. *J. Am. Chem. Soc.* **128,** 1562–1568
23. Chan, A. C., and Carter, P. J. (2010) Therapeutic antibodies for autoimmunity and inflammation. *Nat. Rev. Immunol.* **10,** 301–316
24. Jiang, X. R., Song, A., Bergelson, S., Arroll, T., Parekh, B., May, K., Chung, S., Strouse, R., Mire-Sluis, A., and Schenerman, M. (2011) Advances in the assessment and control of the effector functions of therapeutic antibodies. *Nat. Rev. Drug Discov.* **10,** 101–111
25. Lazar, G. A., Dang, W., Karki, S., Vafa, O., Peng, J. S., Hyun, L., Chan, C., Chung, H. S., Eivazi, A., Yoder, S. C., Vielmetter, J., Carmichael, D. F., Hayes, R. J., and Dahiyat, B. I. (2006) Engineered antibody Fc variants with enhanced effector function. *Proc. Natl. Acad. Sci. U.S.A.* **103,** 4005–4010
26. Page, C. C., Moser, C. C., and Dutton, P. L. (2003) Mechanism for electron transfer within and between proteins. *Curr. Opin Chem. Biol.* **7,** 551–556
27. Page, C. C., Moser, C. C., Chen, X., and Dutton, P. L. (1999) Natural engineering principles of electron tunneling in biological oxidation-reduction. *Nature* **402,** 47–52
28. Horne, C., Klein, M., Polodoulis, I., and Dorrkingtin, K. J. (1982) Noncovalent association of heavy and light chains of human immunoglobulins. III. Specific interactions between VH and VL. *J. Immunol.* **129,** 660–664
29. Goldmacher, V. S., and Kovtun, Y. V. (2011) Antibody-drug conjugates: using monoclonal antibodies for delivery of cytotoxic payloads to cancer cells. *Therapeutic Delivery* **2,** 397–416
30. Ducry, L., and Stump, B. (2010) Antibody-Drug Conjugates: Linking Cytotoxic Payloads to Monoclonal Antibodies. *Bioconjugate Chem.* **21**, 5–13
31. Datta-Mannan, A., Witcher, D. R., Tang, Y., Watkins, J., and Wroblewski, V. J. (2007) Monoclonal antibody clearance. Impact of modulating the interaction of IgG with the neonatal Fc receptor. *J. Biol. Chem.* **282,** 1709–1717
32. Yeung, Y. A. Leabman, M. K., Marvin, J. S., Qiu, J., Adams, C. W., Lien, S. Starovasnik, M. A. and Lowman, H. B. (2009) Engineering human IgG1 affinity to human neonatal Fc receptor: impact of affinity improvement on pharmacokinetics in primates. *J. Immunol.* **182,** 7663–7671
33. Roopenian, D. C., and Akilesh, S. (2007) FcRn: the neonatal Fc receptor comes of age. *Nat. Rev. Immunol.* **7,** 715–725
34. Tabrizi, M. A., Tseng, C. M., and Roskos, L. K. (2006) Elimination mechanisms of therapeutic monoclonal antibodies. *Drug Discov. Today* **11,** 81–88
35. Oganesyan, V., Damschroder, M. M., Leach, W., Wu, H., and Dall'Acqua, W. F. (2008) Structural characterization of a mutated, ADCC-enhanced human Fc fragment. *Mol. Immunol.* **45,** 1872–1882